Formation of a palladium-silicon interface by silane chemical vapor deposition on Pd(100)

C. J. Ennis
Department of Chemistry, University of York, Heslington, York, England

D. J. Spence and S. P. Tear*
Department of Physics, University of York, Heslington, York, England

E. M. McCash
Department of Chemistry, University of York, Heslington, York, England

(Received 2 August 1999)

The utility of chemical vapor deposition of silicon from silane gas as a potential route to interfaces has been investigated on Pd(100) using low-energy electron diffraction and scanning tunneling microscopy. Initial adsorption at room temperature leads to the formation of amorphous palladium silicide/silicon surface layer. Annealing to 650 K after low silane exposure (<5 L) results in subsurface diffusion of silicon with concomitant ejection of palladium atoms. Some surface silicide features also remain intact. Larger exposures (>5 L) at room temperature, followed by 650 K anneal, result in formation of a crystalline $(\sqrt{13}\times\sqrt{13})R33.7°$ silicide reconstruction. This palladium silicide phase is thought to be of Pd_3Si stoichiometry.

I. INTRODUCTION

Metal-semiconductor interfaces are of great importance to the electronics industry in the formation of both Schottky barriers and Ohmic contacts to semiconductor devices. The understanding of how the properties of these interfaces, often different to those of the bulk constituents, arise is a central theme of surface science. As the range of electronic, chemical, structural, and geometrical properties required by various devices is large, an understanding of interface formation and properties is essential to the technological tailoring of devices. This necessity becomes increasingly more acute as device size diminishes and the interfacial region becomes large relative to the body of the device.[1]

The metal-silicon interface is of central importance to silicon integrated circuit technology. All the basic elements of integrated circuits—transistors, diodes, etc.—require extensive interconnections, and termination to external circuits. As well as these Ohmic contacts, metal-silicon interfaces are also required in special applications to act as rectifying Schottky barriers. In a typical medium-sized integrated circuit there are of the order of 500 metal-silicon interfaces, the majority of which act as Ohmic contacts. A small fraction, 10–20%, act as Schottky barriers.[2]

Some metals, e.g., Au, Ag, Al, are unreactive towards silicon surfaces and upon deposition do not form intermetallic silicide compounds. Of these, Al alone is commonly used for Ohmic contacts in VLSI and device applications because it has high adhesive strength with silicon, and a high-eutectic temperature, enabling the contact to survive the often high-fabrication temperatures.[2] However, aluminum contacts are liable to failure in operation due to electromigration of Al atoms in the direction of electron current. Thus, understanding both the structure and dynamics of interfaces as well as seeking suitable interface metals for which electromigratory mechanisms do not significantly affect device performance have become important themes.

Other metals, such as Pt, Pd, and Cu do form silicides upon deposition, and metal silicides have received a great deal of attention due to their metal-like resistivities and their process chemical and thermal stabilities. This leads to their use as materials for low resistivity gates and Ohmic contacts. Mediated by silicide formation a near perfect silicon-metal interface can be formed.[2–4]

Of the silicides used in silicon-metal interfaces, palladium silicide offers several advantages, among which are its relative ease of formation and compatibility with existing process technology, high-temperature morphological stability and shallow junction characteristics (metal rich).[5] Palladium silicide also finds application as a Schottky barrier in solar cells, where the ease of formation makes for cheap, mass producible devices.[6]

Formation of metal silicides is usually carried out by means of metal deposition onto silicon surfaces. Extensive study has been made of the formation of palladium silicide on Si(111).[7–14] In this system, polycrystalline Pd_2Si forms at room temperature and becomes epitaxial after a short anneal above 600 K. Growth proceeds via palladium initially nucleating on the faulted of the Si(111)-(7×7) unit cell, and higher doses lead to the formation of silicide islands. These clusters are uniformly distributed over the substrate surface. The formation of a $(\sqrt{3}\times\sqrt{3})R30°$ phase formed by adsorbed palladium trimers provides the interface between Si(111)-(1×1) and the basal $Pd_2Si(0001)$-(1×1) plane.

The deposition of Pd onto Si(100)-(2×1) (Refs. 7, 11, and 15) surfaces results in the formation of PdSi. Initial room-temperature silicide cluster formation occurs via the Volmer-Weber growth mode, with random nucleation on dimer rows. Annealing results in the formation of square overlayers. At higher exposures Stranski-Krastanov islands form, which exhibit surface features attributable to PdSi unit cells. It is evident from these studies that the silicon substrate morphology has a strong directing effect on silicide formation.

The formation of metal silicide interfaces by the reverse procedure, that of depositing silicon onto the metal surface, displays potential as a route to new structures.[16] The metal substrate offers different electronic and geometrical environments for reaction than does silicon.

Silicon deposition on Pd(110) has been investigated by scanning tunneling microscopy (STM) and reflection-absorption infrared spectroscopy (RAIRS) recently.[17–19] Here, it was found that the substrate temperature during deposition was the main factor in controlling the course of the silicide formation reaction. This reaction competes with silicon sub-surface diffusion. Islands of Pd_2Si form both in the surface and as adislands. These show strain induced misfit dislocations. Similar studies on Pd(100) have revealed the formation of amorphous palladium silicide at temperatures between 150 and 600 K.[20]

Chemical vapor deposition of silicon from silane gas has proved in the past to be a controllable and versatile method of silicide formation.[21–30] We have recently investigated the $Pd(100)/SiH_4$ system in the temperature range 23–200 K using RAIRS,[29] and have found that initial physisorption below 79 K is followed by facile dissociative chemisorption of silane yielding the relatively unusual SiH surface bound species. In the present paper the reaction of silane with Pd(100) at elevated temperatures has been studied by STM and low-energy electron diffraction (LEED).

II. EXPERIMENT

These experiments were carried out in a stainless steel UHV chamber operating at a base pressure of 1×10^{-10} mbar, pumped by an oil diffusion pump and a titanium sublimation pump. The chamber consisted of two stages. The sample preparation stage was equipped with an electron beam heater for sample heating, an argon ion gun, and reverse view LEED optics. The Pd crystal, supplied by Metal Crystals and Oxides Ltd., was cut to the (100) axis ($\pm$ 0.5°). Sample cleaning was achieved by first heating the crystal in oxygen at 650 K followed by cycles of argon-ion sputtering and annealing to 1100 K. Crystal temperature was measured with an infrared pyrometer external to the chamber. Crystal cleanliness was assessed by LEED, sharp (1×1) spots with no (2×1) features from adsorbed CO being taken as indicative of a clean surface.

The STM stage consists of an Omicron STM operating in UHV with polycrystalline tungsten tips prepared by electrochemical etching.

Silane gas, diluted to 0.5% in argon to eliminate explosion risk, was supplied by BOC. Deposition was achieved by backfilling the chamber. All gas exposures are given in Langmuir, and are estimates of the silane dose, not the total gas exposure.

III. RESULTS

3.1 Clean Pd(100)

Figure 1 shows typical STM topographs obtained from the clean Pd(100) surface at room temperature. Large-scale STM images such as Fig. 1(a) show the Pd crystal to exhibit large, flat terrace planes and monatomic step heights. Terrace areas are typically of the order of hundreds of square Ångstroms, and step heights are $1.9\,\text{Å} \pm 0.1\,\text{Å}$, or multiples thereof. This agrees well with the palladium lattice constant, $a = 3.89\,\text{Å}$. Fig. 1(b) shows a typical high resolution scan. In this image the fcc Pd lattice is clearly seen, with a measured lattice constant of $3.9\,\text{Å} \pm 0.3\,\text{Å}$.

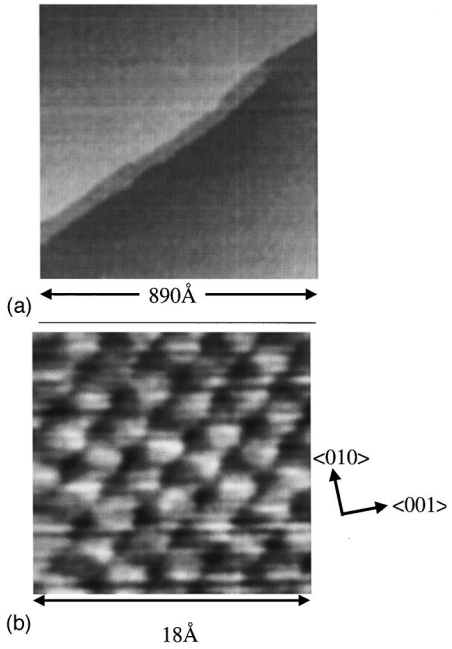

FIG. 1. Clean Pd(100). (a) 2-V sample bias, 2 nA. (b) 0.2-V, 20 nA tunneling current.

3.2 Low exposure

When the crystal is exposed to 1 L silane at room temperature followed by annealing to 650 K, images such as those of Fig. 2 are obtained. The associated LEED pattern shows (1×1) substrate features with a rather high, diffuse background. The large area scan in Fig. 2(a) shows clearly that there has been some considerable modification of the surface. Notably, the surface has become roughened, with both prominences and pits becoming visible. Figure 2(b) shows a typical high-resolution scan of this surface in which four levels are seen: black; dark gray; light gray; and white. The light gray features, which protrude above the dark gray by $0.3\,\text{Å} \pm 0.2\,\text{Å}$, are taken to represent areas where silicon atoms have become incorporated in the surface by reaction with palladium. The bright features in Fig. 2(b) have measured heights of $1.0\,\text{Å} \pm 0.1\,\text{Å}$ and could reasonably represent clusters of palladium atoms that have been ejected from the surface during silicon incorporation.

A competing process to that of silicon incorporation to form a surface silicide is the subsurface diffusion of silicon, typically by a coupled exchange reaction.[17–19] In this process, a palladium atom is spontaneously ejected from the surface, and replaced by a Pd atom from the layer below. This leaves a bulk vacancy, into which a nearby surface-incorporated silicon atom can diffuse. The dark features in Fig. 1(b) are consistent with surface vacancies formed by this process. Generally the bright clusters are preferentially associated with the dark vacancies, which follows, as the ejected palladium is likely to form clusters near the site of ejection.

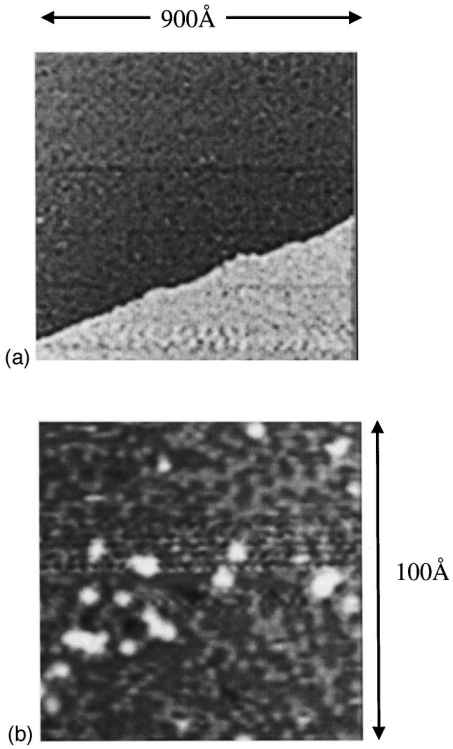

FIG. 2. Pd(100) after exposure to 1 L silane and anneal to 650 K. −1-V sample bias, 0.2 nA tunneling current.

3.3 High exposure

At higher silane exposures (>5 L) the substrate spots in the LEED pattern are totally obscured by the diffuse background. Unpublished RAIRS data that we obtained in a different chamber,[31] combined with this LEED observation indicate that this surface consists of amorphous silicide, consistent with earlier observations of the highly reactive nature of the system.[20,29] Annealing this surface to 650 K for 20 min yields a LEED pattern that, despite the diffuse background, displays a high degree of structure, as shown in Fig. 3(a). Due to our sample shifting slightly in its mount, the incident electron beam was slightly off normal during acquisition of this LEED image, giving rise to some loss of symmetry in diffracted intensities. With this in mind the pattern can be interpreted as a

$$\begin{pmatrix} 3 & -2 \\ 2 & 3 \end{pmatrix}$$

superlattice structure, i.e., $(\sqrt{13}\times\sqrt{13})R33.7°$, a schematic of which is shown in Fig. 3(b). Here, black spots represent substrate reciprocal lattice points, whilst reciprocal lattice points of the two rotated superlattice domains are shown by light and dark gray spots. The second and third order superlattice spots closest to the midpoint of the bulk substrate reciprocal lattice vectors, labeled *A* and *B* in Fig. 3(b), coalesce with those from the other superlattice rotational domain, giving rise to a single elongated spot in Fig. 3(a).

STM investigation of the surface giving rise to this LEED pattern revealed the formation of the large scale islands seen in Fig. 4. The measured height of these islands is 1.7 Å ±0.2 Å. The islands are seen to have an irregular shape and

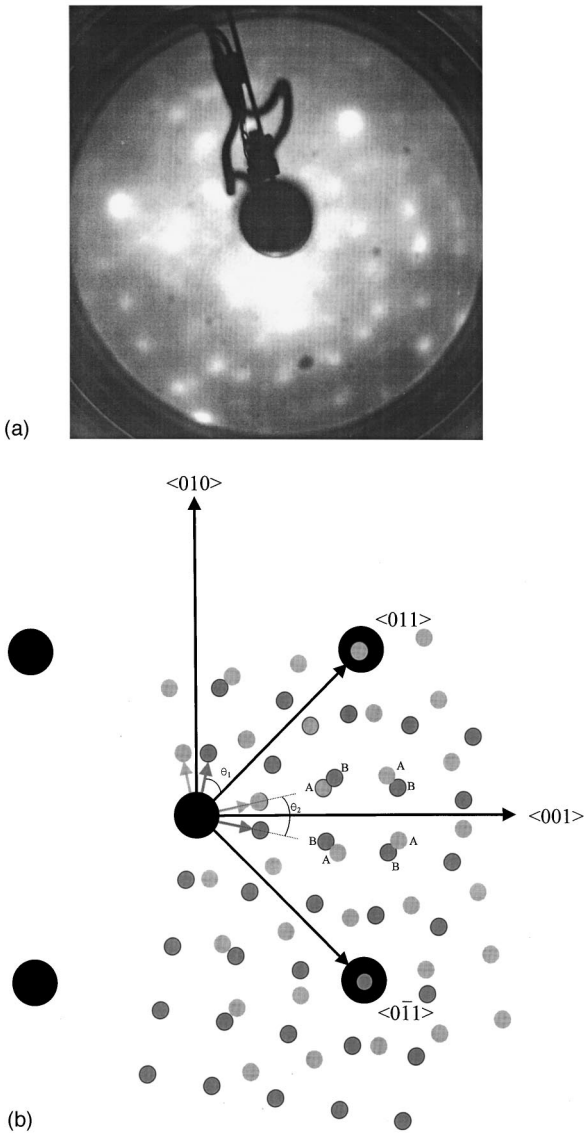

FIG. 3. (a) 70-eV LEED image resulting from >5 L exposure followed by anneal to 650 K. (b) Schematic of LEED image in Fig. 3(a). Black spots represent substrate reflections. Light and dark gray spots represent the two rotated domains of the $(\sqrt{13}\times\sqrt{13})R33.7°$ superstructure. Reciprocal unit vectors and unit cells are also shown. $\theta_1 = 33.7°$, $\theta_2 = 22.6°$.

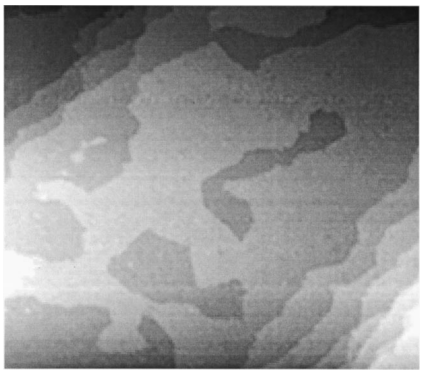

FIG. 4. STM image of surface prepared by >5 L exposure and annealing to 650 K. 2-V sample bias, 2 nA tunneling current.

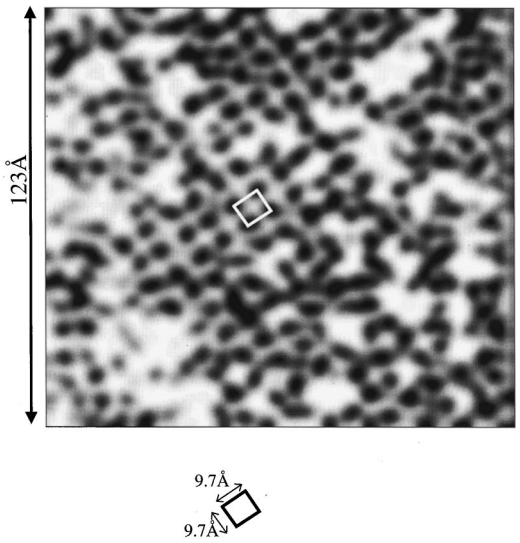

FIG. 5. High-resolution image of surface in Fig. 4. 2-V sample bias, 2 nA tunneling current.

tend to grow out from the step edges. Island growth is to be expected as silane exposure increases. Initially, an extensive layer of amorphous silicide forms on the surface. Annealing activates the back reaction, whereby silicon atoms are released from the silicide. There are then three routes open for these free silicon atoms. They can either: (i) react to form incorporated silicide again; (ii) engage in the coupled exchange diffusion process and go sub-surface or; (iii) diffuse across over the surface and react with clusters of ejected palladium. Via this last process, ejected palladium atoms act as nucleation sites for the growth of islands as silicon diffuses across the surface. The tendency of the ejected palladium atoms to aggregate at step edges causes island growth to occur preferentially from the step edges also.

Figure 5 shows a high-resolution scan of the surface associated with the LEED pattern in Fig. 3. It is clear that the surface has undergone a major reconstruction resulting from the reaction of the palladium substrate with the deposited silicon. This silicide reconstruction has a clearly defined square unit cell of dimensions $9.7\,\text{Å} \pm 0.4\,\text{Å}$. This structure is seen on all terraces, as well as on the surface of the islands, showing that the same structure results from both silicon incorporation and reaction of silicon with ejected palladium. The measured dimensions of this superlattice cell are consistent with those expected for a $(\sqrt{13} \times \sqrt{13})R33.7°$ structure, i.e., 9.9 Å.

Figure 5 also shows the presence of many ill-defined bright features. These are found to be ubiquitous on this surface, and are responsible for the highly diffuse background in the LEED image of Fig. 3(a). STM height information suggests that these features are due to clusters of unreacted palladium.

In the STM image presented in Fig. 6, two domains of the silicide reconstruction are clearly seen. These domains are measured to be rotated by $22° \pm 2°$ with respect to each other. This angular relationship is expected for the $(\sqrt{13} \times \sqrt{13})R33.7°$ structure, in which the domains are rotated $\pm 11.3°$ with respect to the bulk $\langle 001 \rangle$ crystallographic unit vector, giving rise to an angle of 22.6° between domains.

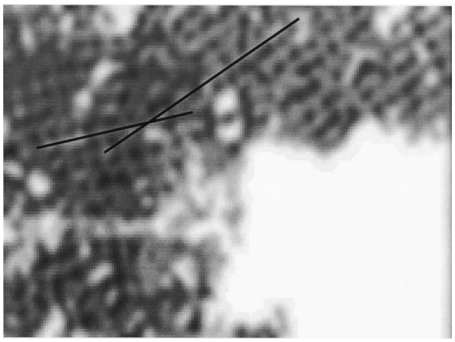

FIG. 6. High-resolution image of the surface in Fig. 4 showing the 22° rotational relationship of the crystalline silicide domains.

IV. DISCUSSION

4.1 Morphology

A striking difference between the current system and that involving Si molecular-beam epitaxy (MBE) on Pd(110) is the apparent thermal stability of the crystalline silicide formed on Pd(100) by silane chemical vapor deposition (CVD) followed by 650 K anneal. The competition between surface reaction and subsurface diffusion has been studied by Walchli *et al.* on Pd(110),[19] and was found to be temperature sensitive. Whilst subsurface diffusion has the lower activation barrier on Pd(110), reaction occurs even at low temperatures (>150 K) and elevated temperatures substantially populate the reaction pathway to form silicide. As the temperature is raised further, however, the silicide thermal decomposition pathway is activated, and the essentially irreversible bulk dissolution acts as a sink for silicon atoms, resulting in the complete loss of surface silicon. This occurs at 550 K on Pd(110). The activation barrier for subsurface diffusion is likely to be higher in the current system due to the greater stability of the (100) surface compared to the (110)—the initial step in the coupled exchange mechanism is the spontaneous ejection of a palladium atom from the surface. That being said however, the low exposure surface [Fig. 2(b)] does show features attributable to subsurface diffusion, indicating that this is an important and active pathway. In the case of Pd(110) the silicide formed is thought to be a strained metastable phase of Pd_2Si. The apparent thermal stability of the crystalline silicide phase formed by silane CVD on Pd(100) may involve a kinetic contribution from the increased activation barrier for subsurface diffusion. Moreover, there seems to be an inherent thermodynamic stability essentially inhibiting the back reaction once the $\sqrt{13}$ structure has formed. The crystallization temperature has not been determined.

Perhaps the most striking difference between the work reported here and previous studies of the reaction of silicon with Pd(100) substrate[20] is that of the formation of a well-defined crystalline silicide. Kern's group deposited silicon atoms from an MBE source directly onto the Pd(100) at temperatures in the range 100 to 600 K and, unlike their work on Pd(110) (Refs. 17–19) failed to observe the formation of anything other than an amorphous silicide. There are three important differences between their work and that which we present here. First, all exposures in our work were carried out at room temperature followed by annealing, in contrast to the previous studies in which exposures were carried out at el-

evated temperatures. This is unlikely to account for the differences seen however, as the formation of the crystalline silicide is thermally activated. Secondly, the anneal temperature in the current work was some 50 K higher than the maximum exposure temperature in the MBE experiment. We have not determined the crystallization temperature of the silicide phase and so it is not possible for us to state conclusively whether this 50 K is critical or not. However, RAIRS experiments we have carried out at low temperature using CO as a probe of surface chemical composition after silane exposure and prior to annealing indicate the presence of both silicide and amorphous silicon.[31] Combined with the observation of the amorphous LEED pattern before annealing this evidence suggests that the surface prepared by decomposition of silane on Pd(100) at room temperature is at least qualitatively similar to that produced by Kern's group by Si MBE at elevated temperatures. This further suggests that annealing to temperatures greater than 600 K *is* needed in order to form the crystalline silicide surface phase. That is, the amorphous silicide/amorphous silicon surface is a nonequilibrium system, and that $T > 600\,\mathrm{K}$ is necessary for establishing of equilibrium and forming the crystalline phase.

This view can be used to rationalize the work conducted so far on the growth of palladium silicides on palladium substrates. On Pd(100), reaction leads initially to the formation of amorphous silicide. Work by Kern's group suggests that this may have Pd_2Si stoichiometry,[20] and has shown its stability with respect to both dissociation and dissolution at temperatures up to 600 K. In our paper, at $T > 600\,\mathrm{K}$ the kinetic barrier to dissociation of amorphous silicide is overcome, liberating silicon and palladium atoms at the surface. The formation of the thermodynamically favored crystalline phase seen in Fig. 5 follows rapidly for high-Si coverage. The competing process of subsurface diffusion by coupled exchange is much less productive than crystallization because: (i) the free energy of the crystalline silicide is presumably much lower than that for bulk dissolved silicon; (ii) further activation is needed i.e. in surface Pd ejection (acting to reduce the rate of dissolution); (iii) under conditions of high coverage the pre-exponential (frequency) factor in Arrhenius kinetics is larger for reaction than for coupled exchange.

Crystallization does not occur at low coverage (resulting from 1 L exposure) on Pd(100), and STM data such as those of Fig. 2 show clear evidence of subsurface diffusion by coupled exchange.[18,19] This can be explained in terms of the above reasoning by noting that in the low-coverage limit significant surface diffusion is required for reaction, and therefore the relative magnitudes of the pre-exponential factors for reaction and subsurface diffusion are reversed compared to the high-coverage scenario. Thus, annealing the low-coverage surface results in significant dissolution of silicon into the bulk along with the reformation of amorphous silicide.

The situation on Pd(110) is different. At relatively low temperatures amorphous silicide is converted into a strained, metastable crystalline phase.[17–19] This is likely to occur due to the more reactive nature of the (110) surface compared to the (100). This reactivity lends either a lower stability (higher free energy) to the Pd(110)/amorphous silicide system, or else provides a reaction path with lower activation energy. Either way, the decomposition of amorphous silicide must be more facile on Pd(110) than on Pd(100). The substrate geometry may well play a role here also. The strain in the crystalline silicide on Pd(110) leads to a lower activation energy for dissociation than that for amorphous silicide on Pd(100), and when dissociation occurs (<600 K) subsurface diffusion is the most active pathway due to the fact that a major reconstruction of the (110) face would be needed in order to form the $\sqrt{13}$ phase of Fig. 5.

As the crystallization temperature of the $\sqrt{13}$ phase has not been determined, the above argument is only conjectural. If further experimentation reveals that formation of the $\sqrt{13}$ phase occurs below 600 K in the case of silane CVD, i.e., its formation is not a continuation of the system studied by Kern's group, then the difference may be ascribed to the third main difference between our work and theirs, namely, the silicon source was different in the two experiments: Si MBE versus CVD with SiH_4. We have good evidence from RAIRS experiments carried out at low temperatures[29] that complete dissociation of silane on Pd(100) occurs well below room temperature, at 200 K and that the liberated hydrogen does not reside on the surface of the palladium.[32] We suggest the hydrogen is absorbed by bulk palladium,[33] and it may well be influencing the reaction in a way not possible with Si MBE. It would be interesting in this respect to compare MBE growth of silicide with and without prior exposure of the Pd(100) to hydrogen.

4.2 Structure

There are five possible scenarios that may account for the STM data presented in Fig. 5. The bulk palladium silicide phase diagram[34] displays four distinct stoichiometries for compound formation: PdSi; Pd_2Si, Pd_9Si_4; and Pd_3Si. Of these, the first two can be discounted as parent structures for the superlattice formed by silane CVD; it is thought unlikely that PdSi should form in this Pd-rich system, while Pd_2Si has an hexagonal unit cell and has been extensively studied in silicide growth by Pd deposition on Si(111)-(7×7).[7–14]

Little is known of the Pd_4Si_9 phase of palladium silicide. It is enticing to note in this respect that the $\sqrt{13}$ unit cell area contains 13 substrate atomic positions, suggesting a relationship with Pd_9Si_4. Pd_3Si exhibits an orthorhombic unit cell but does not possess unit cell dimensions that match those of the current superlattice. It is possible that this is due to our superlattice representing an as yet unstudied surface reconstruction of the bulk compound.

Of all the known palladium silicide stoichiometries, Pd_3Si seems to be the most likely to describe the current silicide superlattice, due to both its residence at the Pd rich end of the Pd-Si phase diagram, and its coexistence with pure Pd in regions of phase space with atom ratios greater than 3:1—attention is drawn to the Pd clusters in Fig. 5. A plausible, yet speculative model for a superlattice of Pd_3Si stoichiometry is presented in Fig. 7. Here, a cluster of nine Pd atoms is decorated by a silicon atom in the central atop position, giving rise to the prominent feature at the intersection of trellis lines in Fig. 5. Four such units joined by silicon atoms in bridginglike positions gives rise to a structure that accounts

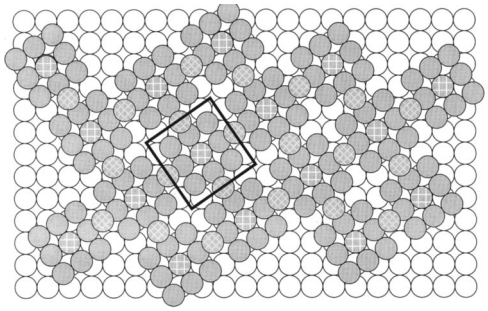

FIG. 7. Proposed model for the Pd_3Si surface stoichiometry. Open circles represent substrate atoms, gray circles represent Pd adatoms, normal hatched circles represent silicon atoms in atop positions, diagonal hatched circles represent silicon atoms in bridginglike positions. Superlattice unit cell based on a cluster of nine Pd adatoms is outlined, demonstrating Pd_3Si stoichiometry.

for the STM image of Fig. 5 taken at face value, i.e., where bright features represent atoms and dark features represent the absence of atoms.

The fifth possible case is one in which the imaged silicide is entirely novel, having neither stoichiometric nor structural relationships with known palladium silicides; this situation has been observed for the formation of silicides by silane CVD on various planes of platinum single crystals.[30]

The Si-Pd system presented here underlines the utility of SiH_4 CVD in the formation of novel interfaces in which the electronic and geometric structure of the metallic substrate plays a crucial role in directing the reaction. Further characterization of the current silicide superlattice using Auger, photoelectron and RAIR spectroscopies will prove fruitful in deducing the detailed chemical and structural nature of this novel interface.

V. CONCLUSION

Chemical vapor deposition of silicon from silane initially yields an amorphous silicide layer on Pd(100). Low exposures lead to silicon incorporation into the surface along with subsurface diffusion via a coupled exchange reaction. High exposure followed by annealing to 650 K results in Stranski-Krastanov island growth with a concomitant large scale reconstruction and gives rise to a novel $(\sqrt{13}\times\sqrt{13})R33.7°$ silicide superlattice. Consideration of the Pd-Si phase diagram and the STM image features leads to a tentative assignment of Pd_3Si stoichiometry to this structure. Pd_3Si stoichiometry has not been observed in any of the systems previously studied, and a Pd_3Si phase with the unit cell dimensions exhibited in the present case has never been observed. The novelty of this silicide underlines the importance of substrate geometry in the growth of interfaces, and the utility of metal substrates in the formation of potentially useful microelectronic device components.

ACKNOWLEDGMENTS

The authors gratefully acknowledge the Engineering and Physical Science Research Council, the University of York Research Priming Fund, and the departments of Physics and Chemistry of the University of York for their support of this work.

*Author to whom correspondence should be addressed. Electronic address: spt1@york.ac.uk

[1] L. J. Brillson, Surf. Sci. **300**, 909 (1993).
[2] J. M. Andrews, J. Vac. Sci. Technol. **11**, 972 (1974).
[3] S. P. Murarka, J. Vac. Sci. Technol. B **4**, 1325 (1986).
[4] G. Ottiaviani and C. Nobili, Thin Solid Films **163**, 111 (1988).
[5] G. W. Rubloff, P. S. Ho, J. F. Freeouf, and J. E. Lewis, Phys. Rev. B **23**, 4183 (1981).
[6] C. Canali, F. Catellani, S. Mantovani, and M. Prudenziati, J. Phys. D **10**, 2481 (1977).
[7] S. Okada, K. Oura, T. Hanawa, and K. Satoh, Surf. Sci. **97**, 88 (1980).
[8] K. Oura, S. Okada, Y. Kishikawa, and T. Hanawa, Appl. Phys. Lett. **40**, 138 (1982).
[9] H. Roux and N. Boutaoui, Surf. Sci. **260**, 113 (1992).
[10] A. A. Kuznetzov, S. Y. Abramova, T. E. Potapova, and O. D. Protopopov, J. Electron Spectrosc. Relat. Phenom. **68**, 407 (1994).
[11] J. F. Chen and L. J. Chen, Thin Solid Films **261**, 107 (1995).
[12] L. Casalis, C. Casati, and M. Kiskinova, Surf. Sci. **331-333**, 381 (1995).
[13] L. Casalis, A. Citti, R. Rosei, and M. Kiskinova, Phys. Rev. B **51**, 1954 (1995).
[14] S. Yoshida, N. Yamamoto, T. Nagamura, M. Oyama, and S. Okazaki, Surf. Sci. **393**, L84 (1997).
[15] H. Itoh, S. Narui, H. Tanabe, and T. Ichinokawa, Surf. Sci. **284**, 236 (1993).
[16] A. Franciosi, Phys. Rev. B **32**, 6917 (1985).
[17] N. Wälchli, E. Kampshoff, and K. Kern, Surf. Sci. **368**, 258 (1996).
[18] N. Wälchli, E. Kampshoff, A. Menck, and K. Kern, Surf. Sci. **382**, L705 (1997).
[19] E. Kampshoff, N. Wälchli, and K. Kern, Surf. Sci. **406**, 103 (1998).
[20] E. Kampshoff, N. Wälchli, and K. Kern, Surf. Sci. **406**, 117 (1998).
[21] L. H. Dubois and R. G. Nuzzo, J. Vac. Sci. Technol. A **2**, 441 (1984).
[22] L. H. Dubois and B. R. Zegarski, Surf. Sci. **204**, 113 (1988).
[23] R. G. Nuzzo and L. H. Dubois, Surf. Sci. **149**, 133 (1985).
[24] A. P. Graham, B. J. Hinch, G. P. Kochanski, E. M. McCash, and W. Allison, Phys. Rev. B **50**, 15 304 (1994).
[25] E. M. McCash, M. A. Chesters, P. Gardner, and S. F. Parker, Surf. Sci. **225**, 273 (1990).
[26] B. C. Weigand, S. P. Lohokare, and R. Nuzzo, J. Phys. Chem. (London) **97**, 11 553 (1993).
[27] A. G. Sault and G. W. Goodman, Surf. Sci. **235**, 28 (1990).
[28] V. Yakovlev, B. Drevillon, N. Layadi, P. Roca, and I. Cabarrocas, J. Appl. Phys. **74**, 2535 (1993).
[29] C. J. Ennis, S. A. Morton, L. Sun, S. P. Tear, and E. M. McCash, Chem. Phys. Lett. **304**, 217 (1999).
[30] J. C. Bondos, N. E. Drummer, A. A. Gewirth, and R. G. Nuzzo, J. Am. Chem. Soc. **121**, 2498 (1999).
[31] Our unpublished RAIRS work revealed a CO stretching band at 2093 cm^{-1} with a high frequency shoulder. This result is similar to that attributed to the presence of amorphous silicide and amorphous silicon in Ref. 20.

[32] In unpublished low temperature RAIRS work on Cu(111) we were able to observe the overtone of the hydrogen bending mode at 1140 cm^{-1}. This band grew in along with the physisorption-chemisorption (dissociative) transition of the silane. No such band was observable in the RAIR spectra of the Pd(100) SiH_4 system. See Ref. 29.

[33] N. N. Greenwood and A. Earnshaw, *Chemistry of the Elements* (Oxford University Press, Oxford, 1984).

[34] *Binary Alloy Phase Diagrams*, 2nd ed. (ASM International, Metals Park, 1986), Vol. 2.